Characterising DARC (Detecting Apoptosing Retinal Cells) spots in glaucoma and healthy eyes

Maddison, John[2]; Choi, Soyoung[1, 2]; Young, Jonathan[2]; Cordeiro, M Francesca[1- 3]

1. Institute of Ophthalmology, University College London, London, London, United Kingdom.
2. Novai Ltd., United Kingdom.
3. Glaucoma & Retinal Neurodegeneration Res Grp, Imperial College, UCL, Western Eye Hsp, United Kingdom.

DISCLOSURES: John Maddison: Commercial Relationship(s); Code P (Patent):Novai Ltd | Soyoung Choi: Commercial Relationship(s);Code E (Employment):Novai Ltd | Jonathan Young: Commercial Relationship(s);Code E (Employment):Novai Ltd | M Francesca Cordeiro: Commercial Relationship(s);Code E (Employment):Novai Ltd;Code C(Consultant/Contractor):Visufarma;Code C (Consultant/Contractor):Allergan;Code C (Consultant/Contractor):Aerie Pharmaceuticals;Code R (Recipient):Novartis;Code F (Financial Support):Santen;Code F (Financial Support):Thea;Code F (Financial Support):Heidelberg Engineering

1. Introduction:

Glaucoma:

Leading cause of irreversible blindness

Unmet need for early identification

Reliable markers for disease prediction, screening and monitoring treatment to be established

DARC Technology:

Fluorescent labelled DARC molecule binds to externalized phosphatidylserine (PS) on the membranes of cells in initial stages of cell stress or apoptosis [1] (Fig.1)

Confocal scanning laser ophthalmoscope used to image the eye to visualise apoptosing cells as fluorescent white spots

Here we analyse the DARC spots identified using the CNN previously described [2-4] from the Phase 2 DARC clinical trial (ISRCTN10751859)

Fig.1

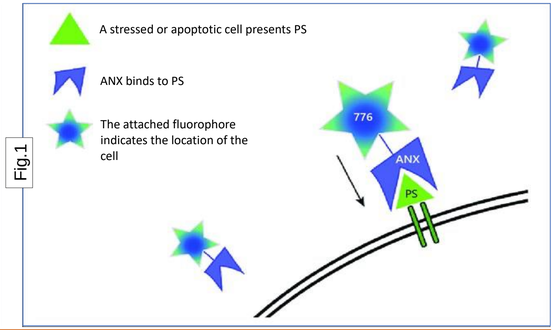

Key Question:

Are there differences in morphological parameters of DARC spots in healthy and glaucoma subjects?

2. Methods:

DARC images

obtained from >40 years glaucoma patient eyes (n=28)
and controls (n=68)

DARC spots

previously developed convolutional neural network - algorithm [2-4]. Fig.2(A)

Descriptive measures (DMs)

per DARC spot defined by shape/intensity characteristics [5-9]

13 DMs were obtained and analysed per spot. Fig.2(B,C)

Statistical analyses

Single and multiple logistic regression over 1000 bootstraps

SLR/MLR Fig.3 (A,B)

Fig 2 (A)

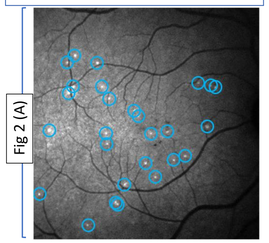

Fig 2 (B)

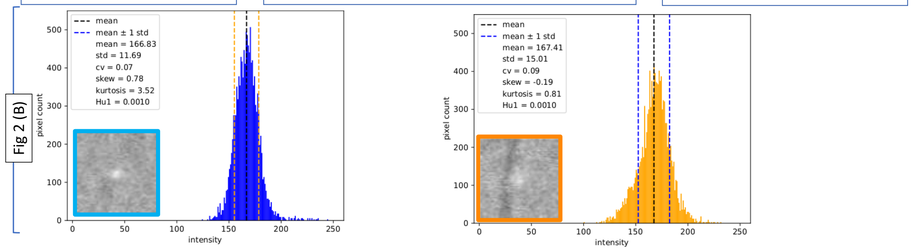

Fig 2 (C)

Mean: Average pixel intensity of a spot [8]

Standard deviation (Std): Variation about the mean[8]

Coefficient of variant (CV): A measure of relative variability (Std/mean) [9]

Skew: Symmetry of histogram [9]

Kurtosis: Flatness of the histogram [8]

Hu moments: moments invariant to translation, scale, rotation and reflection [5,6]

Figure.2
DARC image (A) with automatically identified DARC spots (blue circles, A). DMs obtained from histograms (B) of pixel intensities per spot (insert images, B). Blue = healthy. Orange = glaucoma. Definitions of DMs (C).

3. Results:

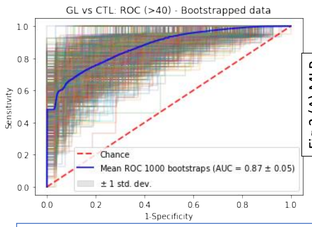

Fig 3 (A) MLR

metric	p-value	hu1	0.043
const	0.36	hu2	0.046
mean	0.609	hu3	0.882
std	0.01	hu4	0.331
cv	0.012	hu5	0.591
skew	0.996	hu6	0.416
kurtosis	0.83	hu7	0.607

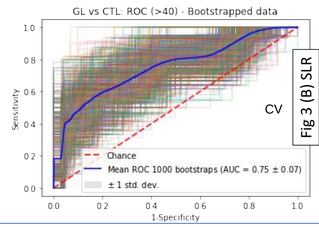

Fig 3 (B) SLR

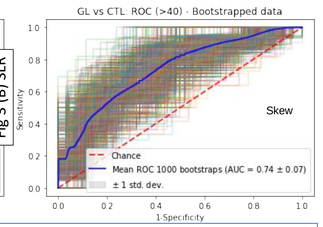

Figure.3
Multiple logistic regression (MLR) with all metrics: results in area under the curve (AUC) of 0.87. The model identifies std, cv, Hu 1 and Hu 2 moments as significant variables (A).
Single logistic regression (SLR) analyses identify cv and skew as best individual metrics with AUCs of 0.75 and 0.74 and p-values of 0.001 and 0.002 respectively (B).

4. Conclusions:

Key message and future implications:
These preliminary results suggest that there are differences in morphological parameters between glaucoma and healthy DARC spots. Further work is needed and more data on definitively differentiating glaucoma disease from health for which we plan to use artificial intelligence to investigate spatial patterns and morphological characteristics to enable further analysis in future, planned clinical trials. Until now, a CNN has only been used to identify DARC labelling.

5. References:

1. Cordeiro MF, Guo L, Luong V, Harding G, Wang W, Jones HE, Moss SE, Sillito AM, Fitzke FW. Real-time imaging of single nerve cell apoptosis in retinal neurodegeneration. Proc Natl Acad Sci U S A. 2004 Sep 7;101(36):13352-6. doi: 10.1073/pnas.0405479101. Epub 2004 Aug 30. PMID: 15340151; PMCID: PMC516570.
2. Normando EM, Yap TE, Maddison J, Miodragovic S, Bonetti P, Almonte M, Mohammad NG, Ameen S, Crawley L, Ahmed F, Bloom PA, Cordeiro MF. A CNN-aided method to predict glaucoma progression using DARC (Detection of Apoptosing Retinal Cells). Expert Rev Mol Diagn. 2020 Jul;20(7):737-748. doi: 10.1080/14737159.2020.1758067. Epub 2020 May 3. PMID: 32310684; PMCID: PMC7115906.
3. Corazza P, Maddison J, Bonetti P, Guo L, Luong V, Garfinkel A, Younis S, Cordeiro MF. Predicting wet age-related macular degeneration (AMD) using DARC (detecting apoptosing retinal cells) AI (artificial intelligence) technology. Expert Rev Mol Diagn. 2021 Jan;21(1):109-118. doi: 10.1080/14737159.2020.1865806. Epub 2020 Dec 28. PMID: 33355491; PMCID: PMC8011474.
4. Cordeiro MF, Hill D, Patel R, Corazza P, Maddison J, Younis S. Detecting retinal cell stress and apoptosis with DARC: Progression from lab to clinic. Prog Retin Eye Res. 2022 Jan;86:100976. doi: 10.1016/j.preteyeres.2021.100976. Epub 2021 Jun 5. PMID: 34102318.
5. Visual Pattern Recognition by Moment Invariants. Hu M.K.. IRE Trans. Info. Theory, vol. IT-8, pp.179–187, 1962
6. Structural Analysis and Shape Descriptors — OpenCV 2.4.13.7 documentation. (2022). Retrieved 14 April 2022, from https://docs.opencv.org/2.4/modules/imgproc/doc/structural_analysis_and_shape_descriptors.html?highlight=cvmatchshapes#humoments
7. Importance of Statistical Measures in Digital Image Processing. Kumar V, Gupta P. IJETAE International Journal of Emerging Technology and Advanced Engineering; Volume 2, Issue 8, August 2012
8. Davnall, F., Yip, C.S.P., Ljungqvist, G. *et al.* Assessment of tumor heterogeneity: an emerging imaging tool for clinical practice?. *Insights Imaging* **3,** 573–589 (2012).
9. Higaki T, Akita K, Katoh K. Coefficient of variation as an image-intensity metric for cytoskeleton bundling. *Sci Rep*. 2020;10(1):22187. Published 2020 Dec 21. doi:10.1038/s41598-020-79136-x